

# Nonlinear standing waves on a periodic array of circular cylinders

Lijun Yuan<sup>1,\*</sup> and Ya Yan Lu<sup>2</sup>

<sup>1</sup>*College of Mathematics and Statistics, Chongqing Technology and Business University, Chongqing 400067, China*

<sup>2</sup>*Department of Mathematics, City University of Hong Kong, Kowloon, Hong Kong*

[\\*yuanlijun.ma@gmail.com](mailto:yuanlijun.ma@gmail.com)

**Abstract:** A periodic array of parallel and infinitely long dielectric circular cylinders surrounded by air can be regarded as a simple two-dimensional periodic waveguide. For linear cylinders, guided modes exist continuously below the lightline in various frequency intervals, but standing waves, which are special guided modes with a zero Bloch wavenumber, could exist above the lightline at a discrete set of frequencies. In this paper, we consider a periodic array of nonlinear circular cylinders with a Kerr nonlinearity, and show numerically that nonlinear standing waves exist continuously with the frequency and their amplitudes depend on the frequency. The amplitude-frequency relations are further investigated in a perturbation analysis.

© 2015 Optical Society of America

**OCIS codes:** (190.0190) Nonlinear optics; (190.3270) Kerr effect; (000.4430) Numerical approximation and analysis; (050.1755) Computational electromagnetic methods.

---

## References and links

1. S. Peng, T. Tamir, and H. Bertoni, "Theory of periodic dielectric waveguides," *IEEE Trans. Microw. Theory Techn.* **23**(1), 123–133 (1975).
2. S. Fan, J. N. Winn, A. Devenyi, J. C. Chen, R. D. Meade, and J. D. Joannopoulos, "Guided and defect modes in periodic dielectric waveguides," *J. Opt. Soc. Am. B* **12**(7), 1267–1272 (1995).
3. A. Yariv, Y. Xu, R. K. Lee, and A. Scherer, "Coupled resonator optical waveguide: a proposal and analysis," *Opt. Lett.* **24**, 711–713 (1999).
4. S. G. Johnson, P. R. Villeneuve, S. Fan, and J. D. Joannopoulos, "Linear waveguides in photonic-crystal slabs," *Phys. Rev. B* **62**, 8212–8222 (2000).
5. D. N. Chigrin, A. V. Lavrinenko, and C. M. Sotomayor Torres, "Nanopillars photonic crystal waveguides," *Opt. Express* **12**, 617–622 (2004).
6. A.-S. Bonnet-Bendhia and F. Starling, "Guided waves by electromagnetic gratings and nonuniqueness examples for the diffraction problem," *Math. Meth. Appl. Sci.* **17**, 305–338 (1994).
7. H. D. Maniar and J. N. Newman, "Wave diffraction by a long array of cylinders," *J. Fluid Mech.* **339**, 309–330 (1997).
8. D. V. Evans and R. Porter, "Trapped modes embedded in the continuous spectrum," *Quart. J. Mech. Appl. Math.* **51**(2), 263–274 (1998).
9. R. Porter and D. V. Evans, "Embedded Rayleigh-Bloch surface waves along periodic rectangular arrays," *Wave Motion* **43**, 29–50 (2005).
10. S. Shipman and D. Volkov, "Guided modes in periodic slabs: existence and nonexistence," *SIAM J. Appl. Math.* **67**, 687–713 (2007).
11. D. C. Marinica, A. G. Borisov, and S. V. Shabanov, "Bound states in the continuum in photonics," *Phys. Rev. Lett.* **100**, 183902 (2008).
12. Y. Plotnik, O. Peleg, F. Dreisow, M. Heinrich, S. Nolte, A. Szameit, and M. Segev, "Experimental observation of optical bound states in the continuum," *Phys. Rev. Lett.* **107**, 183901 (2011).
13. M. I. Molina, A. E. Miroshnichenko, and Y. S. Kivshar, "Surface bound states in the continuum," *Phys. Rev. Lett.* **108**, 070401 (2012).

14. J. Lee, B. Zhen, S. Chua, W. Qiu, J. D. Joannopoulos M. Soljačić, and O. Shapira, "Observation and differentiation of unique high-Q optical resonances near zero wave vector in macroscopic photonic crystal slabs," *Phys. Rev. Lett.* **109**, 067401 (2012).
15. C. W. Hsu, B. Zhen, S.-L. Chua, S. G. Johnson, J. D. Joannopoulos, and M. Soljačić, "Bloch surface eigenstates within the radiation continuum," *Light Sci. Appl.* **2**, e84 (2013).
16. C. W. Hsu, B. Zhen, J. Lee, S.-L. Chua, S. G. Johnson, J. D. Joannopoulos, and M. Soljačić, "Observation of trapped light within the radiation continuum," *Nature* **499**, 188-191 (2013).
17. B. Zhen, C. W. Hsu, L. Lu, A. D. Stone, and M. Soljačić, "Topological nature of optical bound states in the continuum," *Phys. Rev. Lett.* **113**, 257401 (2014).
18. Z. Hu and Y. Y. Lu, "Standing waves on two-dimensional periodic dielectric waveguides," *J. Opt.* **17**(6), 065601 (2015).
19. N. D. Sankey, D. F. Prelewitz, and T. G. Brown, "All-optical switching in a nonlinear periodic-waveguide structure," *Appl. Phys. Lett.* **60**, 1427-1429 (1992).
20. M. F. Yanik, S. Fan, and M. Soljačić, "High-contrast all-optical bistable switching in photonic crystal microcavities," *Appl. Phys. Lett.* **83**, 2739-2741 (2003).
21. N. C. Panoiu, M. Bahl, and R. M. Osgood, Jr. "All-optical tunability of a nonlinear photonic crystal channel drop filter," *Opt. Express* **12**(8) 1605-1610 (2004).
22. C. A. Stuart, "Guidance properties of nonlinear planar waveguides," *Arch. Ration. Mech. Anal.* **125**, 145-200 (1993).
23. H. W. Schürmann, V. S. Serov, and Y. V. Shestopalov, "TE polarized waves guided by a lossless nonlinear three-layer structure," *Phys. Rev. E* **58**(1), 1040-1050 (1998).
24. D. V. Valovik, "Propagation of electromagnetic waves in a nonlinear metamaterial layer," *J. Commun. Technol. and Electron.* **56**(5), 544-556 (2011).
25. D. V. Valovik and Y. G. Smirnov, "Nonlinear effects in the problem of propagation of TM electromagnetic waves in a Kerr nonlinear layer," *J. Commun. Technol. and Electron.* **56**(3), 283-288 (2011).
26. Y. G. Smirnov and D. V. Valovik, "Guided electromagnetic waves propagating in a plane dielectric waveguide with nonlinear permittivity," *Phys. Rev. A* **91**, 013840 (2015).
27. H. W. Schürmann, G. Yu. Smirnov, and V. Yu. Shestopalov, "Propagation of te-waves in cylindrical nonlinear dielectric waveguides," *Phys. Rev. E* **71**(1), 016614 (2005).
28. Y. Smirnov, H. W. Schürmann, and Y. Shestopalov, "Integral equation approach for the propagation of TE-waves in a nonlinear dielectric cylindrical waveguide," *J. Nonlinear Math. Phys.* **11**(2), 256-268 (2004).
29. S. F. Mingaleev and Y. S. Kivshar, "Nonlinear transmission and light localization in photonic-crystal waveguides," *J. Opt. Soc. Am. B* **19**, 2241-2249 (2002).
30. B. Maes, P. Bienstman, and R. Baets, "Bloch modes and self-localized waveguides in nonlinear photonic crystals," *J. Opt. Soc. Am. B* **22**(3), 613-619 (2005).
31. T. Fujisawa and M. Koshiba "Finite-element mode-solver for nonlinear periodic optical waveguides and its application to photonic crystal circuits," *J. Lightwave Technol.* **23**(1), 382-387 (2005).
32. I. S. Maksymov, L. F. Marsal, and J. Pallarès, "An FDTD analysis of nonlinear photonic crystal waveguides," *Opt. Quant. Electron.* **38**, 149-160 (2006).
33. R. W. Boyd, *Nonlinear Optics*, 3rd ed. (Academic, 2008).
34. D. C. Marinica, A. G. Borisov, and S. V. Shabanov, "Second harmonic generation from arrays of subwavelength cylinders," *Phys. Rev. B* **76**, 085311 (2007).
35. F. R. Ndangali and S. V. Shabanov, "The resonant nonlinear scattering theory with bound states in the radiation continuum and the second harmonic generation," *Proc. of SPIE* **8808**, 88081F (2013).
36. L. Yuan and Y. Y. Lu, "Efficient numerical method for analyzing optical bistability in photonic crystal microcavities," *Opt. Express* **21**, 11952-11964 (2013).
37. L. Yuan and Y. Y. Lu, "Bilateral symmetry breaking in nonlinear circular cylinders," *Opt. Express* **22**, 30128-30136 (2014).
38. L. N. Trefethen, *Spectral Methods in MATLAB* (Society for Industrial and Applied Mathematics, 2000).
39. L. Yuan and Y. Y. Lu, "Analyzing second harmonic generation from arrays of cylinders using Dirichlet-to-Neumann maps," *J. Opt. Soc. Am. B* **26**(4), 587-594 (2009).

---

## 1. Introduction

Dielectric waveguides with a periodicity along the waveguide axis are important for practical applications and have been studied by many authors [1-5]. A guided mode of a linear lossless periodic waveguide is a Bloch mode with a real wavenumber and a periodic mode profile that decays exponentially to zero in the transverse directions. If the waveguide core is surrounded by a homogeneous medium, guided modes usually exist continuously below the lightline. Above the lightline, there is a continuum of radiation modes, thus it is difficult to localize the wave field

around the waveguide core. Nevertheless, guided modes could exist above the lightline under various conditions [6–18]. In particular, if the periodic waveguide has a reflection symmetry along its axis, the existence of standing waves (which are special guided modes with a zero wavenumber) is well known. For two-dimensional (2D) waveguides, it appears that guided modes above the lightline can only exist at a discrete set of frequencies.

Nonlinear effects due to the Kerr nonlinearity can be useful for applications such as all-optical switching [19, 20] and filtering [21]. Guided modes in nonlinear waveguides have been studied by many authors [22–32]. Most of these studies [22–27] are concerned with waveguides that are invariant along their axes. The nonlinear guided modes in these waveguides exist below the lightline. For photonic crystal waveguides [29–32], nonlinear guided modes are confined around the waveguide core by the bandgap effect. To the best of our knowledge, for waveguides with a homogeneous medium surrounding the core, nonlinear guided modes above the lightline have never been studied.

In this paper, we analyze a very simple nonlinear periodic waveguide: a periodic array of circular cylinders surrounded by air where the cylinders have a Kerr nonlinearity. Using a highly accurate numerical method, we calculate nonlinear standing waves and show their continuous dependence on the frequency. These standing waves are special guided modes with a zero wavenumber, are periodic along the array, and decay exponentially to zero in the transverse direction. Similar to the linear case, the existence of these nonlinear standing modes are protected by a reflection symmetry of the array. The amplitudes of the nonlinear standing waves depend on the frequency. An explicit and approximate relation between the amplitude and the frequency is derived by a perturbation method, and it is valid when the amplitude is small and the frequency is close to that of a linear standing wave. The existence of guided modes above the lightline is closely related to the non-uniqueness of the related diffraction problem where a plane incident wave impinges on the waveguide [6]. For linear problems, the diffraction problem has no uniqueness for a discrete set of frequencies. Our numerical results indicate that for nonlinear problems, the diffraction problem may lose uniqueness for all frequencies within a relevant interval.

## 2. Problem formulation

We consider a periodic array of parallel and infinitely long circular dielectric cylinders surrounded by air as shown in Fig. 1. The period of the array (i.e., the center-to-center distance

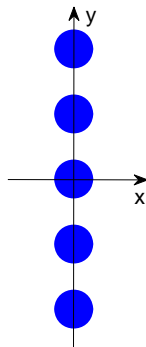


Fig. 1. A periodic array of circular cylinders of radius  $a$  with a period  $L$  in the  $y$  direction.

between two nearby cylinders) is  $L$ . The refractive index and the radius of the cylinders are  $n_1$  and  $a$ , respectively, where  $n_1 > 1$  and  $a < L/2$ . The cylinders are made of a nonlinear material

with a Kerr nonlinearity. In a Cartesian coordinate system  $\{x, y, z\}$ , we assume the cylinders are parallel to the  $z$  axis, and the centers of the cylinders in the  $xy$  plane are located at  $(0, jL)$  for all integers  $j$ . The array acts as a 2D periodic waveguide with its axis in the  $y$  direction. Since the origin is located at the center of one cylinder, the structure is symmetric with respect to both  $x$  and  $y$  axes.

For the  $E$  polarization, the governing equation in the time domain is the following nonlinear wave equation [33]

$$\frac{\partial^2 E_z}{\partial x^2} + \frac{\partial^2 E_z}{\partial y^2} - \frac{n^2}{c^2} \frac{\partial^2 E_z}{\partial t^2} - \frac{\chi^{(3)}}{c^2} \frac{\partial^2 E_z^3}{\partial t^2} = 0, \quad (1)$$

where  $E_z$  is the  $z$  component of the actual real electric field,  $c$  is the speed of light in vacuum,  $n = n(x, y)$  is the refractive index function satisfying  $n = n_1$  in the cylinders and  $n = n_0 = 1$  outside the cylinders,  $\chi^{(3)} = \chi^{(3)}(x, y)$  is an element of the third order nonlinear susceptibility tensor and it is zero outside the cylinders. Assuming the wave field is associated with a fundamental angular frequency  $\omega$ , we expand  $E_z$  in harmonic waves as

$$E_z = \text{Re} [u_1 e^{-i\omega t} + u_3 e^{-3i\omega t} + \dots], \quad (2)$$

where  $u_1$  and  $u_3$  are the complex amplitudes of the first and third order harmonic waves. Substituting Eq. (2) into Eq. (1) and ignoring the high order harmonics, we obtain the following nonlinear Helmholtz equation for the fundamental frequency wave

$$\frac{\partial^2 u}{\partial x^2} + \frac{\partial^2 u}{\partial y^2} + k_0^2 (n^2 + \gamma |u|^2) u = 0, \quad (3)$$

where  $u$  is used to denote  $u_1$  for simplicity,  $k_0 = \omega/c$  is the free space wavenumber, and  $\gamma = \frac{3}{4} \chi^{(3)}$  is the nonlinear coefficient which vanishes in linear media. In the nonlinear cylinders, we assume  $\gamma = \gamma_1 > 0$ . We remark that it is not always possible to ignore the third and higher harmonics. From related studies on second harmonic generation [34, 35], we expect that third harmonic generation becomes important when some resonance conditions are satisfied. In that case, it is necessary to consider a coupled system of nonlinear Helmholtz equations for  $u_1$ ,  $u_3$ , etc. Nevertheless, we believe Eq. (3) is valid for the majority of cases where the resonance conditions are not satisfied.

A nonlinear guided mode of such a periodic waveguide is a solution of Eq. (3) given as

$$u(x, y) = U(x, y) e^{i\beta y}, \quad (4)$$

where  $U$  is periodic in  $y$  with period  $L$  and decays exponentially to zero as  $|x| \rightarrow \infty$ , and  $\beta$  is the real Bloch wavenumber. Typically, guided modes exist below the lightline, that is, the Bloch wavenumber satisfies  $\beta > k_0 n_0$ . A standing wave is a special guided mode with  $\beta = 0$ . In that case,  $u$  itself is periodic in  $y$  with period  $L$ , i.e.,

$$u(x, y + L) = u(x, y) \quad (5)$$

and it decays to zero exponentially as  $|x| \rightarrow \infty$ . Clearly, a standing wave (defined using the minimum period  $L$ ) is a solution above the lightline.

Since  $u$  is periodic in the  $y$  direction, it can be expanded in Fourier series as

$$u(x, y) = \begin{cases} \sum_{m=-\infty}^{+\infty} b_m^+ e^{i(\alpha_m x + \beta_m y)}, & x > L/2 \\ \sum_{m=-\infty}^{+\infty} b_m^- e^{i(-\alpha_m x + \beta_m y)}, & x < -L/2 \end{cases} \quad (6)$$

where  $\beta_m = 2\pi m/L$  and  $\alpha_m = \sqrt{k_0^2 n_0^2 - \beta_m^2}$ . The  $x$  dependence in the above expansion is chosen so that each term is either outgoing or exponentially decaying as  $|x| \rightarrow \infty$ . If the frequency  $\omega$  satisfies  $\omega L/(2\pi c) < 1$ , then  $\alpha_0 > 0$  and all other  $\alpha_m$  for  $m \neq 0$  are pure imaginary. In that case, to ensure that  $u$  decays to zero as  $|x| \rightarrow \infty$ , we only need the condition  $b_0^\pm = 0$ . Notice that if  $u$  is an odd function of  $y$ , i.e.  $u(x, y) = -u(x, -y)$ , then this condition is automatically satisfied. We restrict our study to frequencies satisfying  $\omega L/(2\pi c) < 1$  and consider odd solutions. This allows us to reduce the computation domain to half a period, i.e. for  $0 < y < L/2$ , with zero boundary conditions  $u = 0$  at  $y = 0$  and  $y = L/2$ . Since the structure is also symmetric with respect to the  $y$  axis, i.e.  $n(x, y) = n(-x, y)$ , we can separately consider solutions that are even or odd in the  $x$  direction. Therefore, the computation domain can be further reduced to one quarter of the period, i.e. for  $x > 0$  and  $0 < y < L/2$ . At  $x = 0$ , the boundary conditions for the even and odd solutions are  $\partial_x u = 0$  and  $u = 0$ , respectively.

The problem formulated above for nonlinear standing waves on the array of cylinders is an eigenvalue problem, where  $u$  is the eigenfunction and  $k_0^2$  (or  $k_0$ , related to the frequency  $\omega$ ) is the eigenvalue. Notice that a trivial solution is  $u \equiv 0$  and we are looking for non-trivial solutions. However, this is a nonlinear eigenvalue problem. While the related linear eigenvalue problem for  $\gamma = 0$  has a discrete set of eigenvalues and the corresponding eigenfunctions have arbitrary amplitudes, the nonlinear eigenvalue problem seems to have continuous eigenvalues and the amplitude of an eigenfunction depends on the eigenvalue.

A solution of the nonlinear Helmholtz Eq. (3) is in general a complex-valued function. This is necessary to represent propagating waves with the time dependence  $e^{-i\omega t}$ . Since the standing waves are non-propagating, it is possible to have real solutions. Besides, since the nonlinear eigenvalue problem is homogeneous, if  $u$  is a solution, then  $u$  multiplies any complex number with unit magnitude is also a solution. For simplicity, we restrict ourself to real solutions.

### 3. Numerical method

To systematically find the nonlinear standing waves, an efficient and highly accurate numerical method is needed. To take advantage of the circular geometry of the cylinders, we develop a special numerical method that reduces the computation domain to the disk  $D$  corresponding to the cross section of a cylinder and solves the nonlinear Helmholtz equation on  $D$ . More precisely, our numerical method involves four steps: 1) reduce the computation domain to a square  $\Omega$ ; 2) further reduce the computation domain to the disk  $D$ ; 3) discretize the nonlinear Helmholtz equation by a mixed Chebyshev-Fourier pseudospectral method; 4) solve the discretized nonlinear system of equations by an iterative method. In the above, the square  $\Omega = \{(x, y) : |x| < L/2, |y| < L/2\}$  corresponds to one period in the  $y$  direction and a truncation of length  $L$  in the  $x$  direction. The disk  $D$  is given by  $r < a$ , where  $r$  is the radial variable of the polar coordinate system.

Since  $u$  is periodic in  $y$ , we can obviously reduce the problem to one period, i.e., the trip given by  $-L/2 < y < L/2$  and  $-\infty < x < \infty$ . The periodic boundary condition Eq. (5) gives rise to

$$u(x, -L/2) = u(x, L/2), \quad (7)$$

$$\frac{\partial u}{\partial y}(x, -L/2) = \frac{\partial u}{\partial y}(x, L/2). \quad (8)$$

To truncate the  $x$  variable, we make use of the Fourier series given in Eq. (6). Although the coefficients  $b_m^\pm$  are unknown, if we define a linear operator  $\mathbf{T}$  satisfying

$$\mathbf{T}e^{i\beta_m y} = i\alpha_m e^{i\beta_m y} \quad \text{for} \quad -\infty < m < +\infty, \quad (9)$$

then

$$\frac{\partial u}{\partial x} = \pm \mathbf{T}u \quad \text{at } x = \pm L/2. \quad (10)$$

Notice that the operator  $\mathbf{T}$  depends on  $k_0$ . With the boundary conditions Eqs. (7), (8) and (10), we only need to solve Eq. (3) in the square  $\Omega$ . If each edge of  $\Omega$  is discretized by  $N$  points, then  $\mathbf{T}$  can be approximated by an  $N \times N$  matrix.

It is useful to further reduce the computation domain to the disk  $D$  which corresponds the cross section of the nonlinear cylinder in  $\Omega$ . Equation (3) is a nonlinear partial differential equation, but it is only nonlinear in  $D$ . Due to the nonlinearity, Eq. (3) can only be solved by an iterative method. As shown in our previous works on optical bistability [36] and symmetry breaking [37], when the computation domain is reduced, the iterations can be performed more efficiently, and it is also easier to achieve a convergence. To reduce the computation domain from  $\Omega$  to  $D$ , we consider the domain outside  $D$  and inside  $\Omega$ , i.e.  $Q = \Omega \setminus \bar{D}$ , where Eq. (3) becomes linear. Using the cylindrical wave expansion of  $u$  in  $Q$ , we can find an operator  $\Lambda$ , the so-called Dirichlet-to-Neumann (DtN) map, such that

$$\Lambda \begin{bmatrix} u(x, L/2) \\ u(x, -L/2) \\ u(L/2, y) \\ u(-L/2, y) \\ u|_{\partial D} \end{bmatrix} = \begin{bmatrix} \partial_y u(x, L/2) \\ \partial_y u(x, -L/2) \\ \partial_x u(L/2, y) \\ \partial_x u(-L/2, y) \\ \partial_r u|_{\partial D} \end{bmatrix}, \quad (11)$$

where  $\partial D$  is the boundary of  $D$ , i.e., the circle  $r = a$ . Notice that the boundary of  $Q$  consists of four edges of  $\Omega$  and the circle  $\partial D$ . The operator  $\Lambda$  maps  $u$  to the normal derivative of  $u$  on the boundary of  $Q$ . If we can discretize each edge of  $\Omega$  by  $N$  points and discretize the circle  $\partial D$  by  $4N$  points, then  $\Lambda$  can be approximated by a  $(8N) \times (8N)$  matrix. Combining the boundary conditions Eqs. (7), (8), (10) with Eq. (11), we can find a boundary condition on  $\partial D$ :

$$\frac{\partial u}{\partial r} = \mathbf{B}(k_0)u \quad \text{at } r = a, \quad (12)$$

where  $\mathbf{B}$  is an operator and it depends on  $k_0$ . Using the same discretization,  $\mathbf{B}$  is approximated by a  $(4N) \times (4N)$  matrix. Therefore, we only need to solve the nonlinear Helmholtz Eq. (3) in  $D$  together with the boundary condition Eq. (12). Furthermore, as discussed in section 2,  $u$  is an odd function of  $y$ , and it is either even or odd in  $x$ . Using these symmetries, we can reduce the computation domain to one quarter of  $D$ .

Since the nonlinear standing waves seem to exist for all frequencies satisfying  $\omega L / (2\pi c) < 1$ , we calculate  $u$  for each given  $k_0$ . It is useful to introduce the amplitude  $A$  of a standing wave, such that

$$u(x, y) = Aw(x, y) \quad (13)$$

with  $|w(x, y)| \leq 1$  for all  $(x, y)$  and  $\max w(x, y) = 1$ . In disk  $D$ , Eq. (3) is then written as

$$\frac{\partial^2 w}{\partial x^2} + \frac{\partial^2 w}{\partial y^2} + k_0^2 (n^2 + \gamma_1 A^2 w^2) w = 0. \quad (14)$$

In the above, we have replaced  $|w|^2$  by  $w^2$ , because we assume  $u$  is real. Equation (14) can be discretized by a mixed Chebyshev-Fourier pseudospectral method [38]. If we use  $4N$  and  $M$  points to discretize the angular and radial variables of  $D$ , respectively, then Eq. (14) and boundary condition Eq. (12) are approximated by the following system of nonlinear algebra equations

$$\mathbf{N}(k_0)\mathbf{w} + k_0^2 \gamma_1 A^2 \mathbf{w}^3 = \mathbf{0}, \quad (15)$$

where  $\mathbf{N}$  is a  $(4NM) \times (4NM)$  matrix related to the differential operator  $\partial_x^2 + \partial_y^2 + k_0^2 n^2$  and boundary condition Eq. (12),  $\mathbf{w}$  is a column vector for  $w$  at the  $4NM$  grid points,  $\mathbf{w}^3$  is the element-wise cubic power of  $\mathbf{w}$ . More details on the mixed Chebyshev-Fourier pseudospectral method can be found in [38] and [39]. Notice that the matrix  $\mathbf{N}$  depends on  $k_0$ .

Equation (15) can be solved by Newton's method. If  $\mathbf{w}_j$  and  $A_j$  are the given  $j$ th iteration, we first calculate  $\mathbf{w}_{j+1}$  from

$$[\mathbf{N}(k_0) + 3k_0^2 \gamma_1 A_j^2 \mathbf{w}_j^2] \mathbf{w}_{j+1} = 2k_0^2 \gamma_1 A_j^2 \mathbf{w}_j^3, \quad (16)$$

then re-normalize  $\mathbf{w}_{j+1}$  such that  $\max \mathbf{w}_{j+1} = 1$ . The squared amplitude of the  $(j+1)$ st iteration is then given by

$$A_{j+1}^2 = \frac{-\mathbf{w}_{j+1}^T \mathbf{N}(k_0) \mathbf{w}_{j+1}}{k_0^2 \gamma_1 \mathbf{w}_{j+1}^T \mathbf{w}_{j+1}^3}, \quad (17)$$

where the superscript "T" denotes the transpose operation. To start the iterative process, initial values for  $\mathbf{w}_0$  and  $A_0$  are needed.

#### 4. Results

We consider a periodic array of nonlinear circular cylinders with radius  $a = 0.3L$ , refractive index  $n_1 = 2.5$ , and a third order nonlinear coefficient  $\chi^{(3)} = (8/3) \times 10^{-12} \text{ m}^2/\text{V}^2$ , i.e.  $\gamma_1 = 2 \times 10^{-12} \text{ m}^2/\text{V}^2$ . The nonlinear cylinders are surrounded by air. The case for a linear array of circular cylinders has been systematically studied in [18]. There are two linear standing waves at frequencies  $\omega L/(2\pi c) \approx 0.5502$  and  $0.7800$ , and their wave field patterns are shown in Fig. 2.

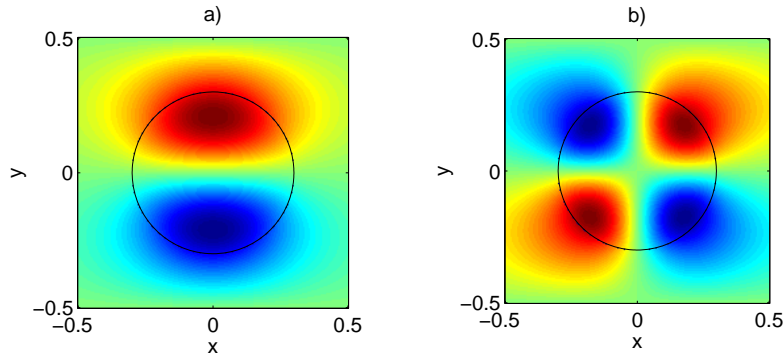


Fig. 2. Electric field patterns of the two linear standing waves for a periodic array of circular cylinders with radius  $a = 0.3L$  and refractive index  $n_1 = 2.5$ . a) for frequency  $(\omega L)/(2\pi c) \approx 0.5502$ ; b) for frequency  $(\omega L)/(2\pi c) \approx 0.7800$ .

For the nonlinear case, using the numerical method presented in the previous section, we found many nonlinear standing waves for frequencies satisfying  $\omega L/(2\pi c) < 1$ . In Fig. 3, we show the amplitude-frequency relations for the first seven standing waves, where the vertical axis is the scaled amplitude  $|A|\sqrt{\gamma_1}$ . In general, the amplitude of a nonlinear standing wave increases as the frequency is decreased. When the frequency approaches zero, the amplitude must tend to infinity, because otherwise the solution will satisfy the Laplace equation ( $\partial_x^2 u + \partial_y^2 u = 0$ )

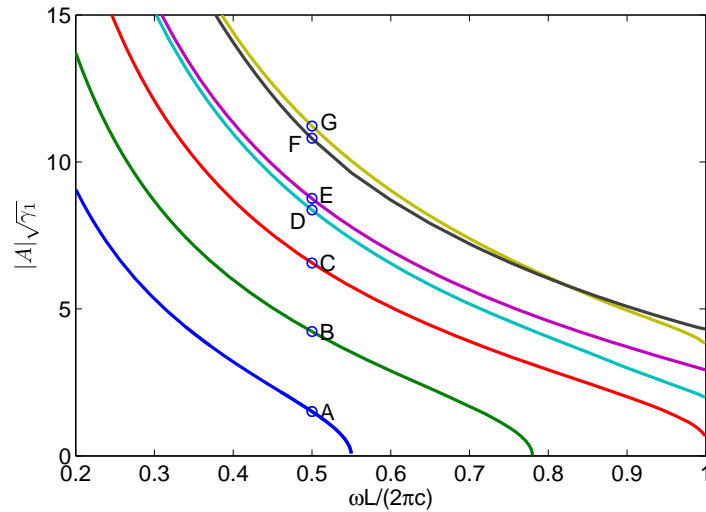


Fig. 3. Amplitude-frequency relations of seven nonlinear standing waves on a periodic array of circular nonlinear cylinders.

which has only a zero solution for the given boundary conditions. Notice that the two lowest curves (i.e. the curves with points marked A and B) are connected to the frequencies of the two linear standing waves, as the amplitude tends to zero. All other curves disappear at  $\omega L/(2\pi c) = 1$ . This is because when  $\omega L/(2\pi c) > 1$ ,  $\alpha_1$  in Eq. (6) is positive, but the coefficients  $b_1^\pm$  in the Fourier expansions are nonzero in general. We also note that the two highest curves (i.e. the curves with points marked F and G) intersect at frequency  $\omega L/(2\pi c) \approx 0.82$ . However, the two nonlinear standing waves at this intersection are completely different, and they just have the same amplitudes.

In Fig. 4, we show the electric field patterns of the seven nonlinear standing waves at  $\omega L/(2\pi c) = 0.5$ , corresponding to points A to G in Fig. 3. The first two field patterns (for points A and B, respectively) are very similar to those of the linear standing waves shown in Fig. 2. This is as expected, because they are on the two lowest curves that connect to the linear standing waves. The symmetries of these nonlinear standing waves can be easily observed from the plots. We can see that  $u$  is anti-symmetric along the vertical direction, i.e.  $u$  is an odd function of  $y$ . In fact, we have  $u = 0$  on horizontal lines at  $y = 0$  and  $y = \pm L/2$ . As a result, the zeroth order coefficients  $b_0^\pm$  in the Fourier expansion Eq. (6) are zero. Thus, the wave field truly decays to zero exponentially, as  $|x| \rightarrow \infty$ . With respect to the  $x$  direction, a nonlinear standing wave is either symmetric (an even function of  $x$ ) or anti-symmetric (an odd function of  $x$ ).

Although only seven nonlinear standing waves are shown, we believe there are infinite number of them for any frequency satisfying  $\omega L/(2\pi c) < 1$ . For the linear array with a fixed radius  $a$  and refractive index  $n_1$ , there are a finite number of standing waves, but that number increases as  $n_1$  is increased [18]. In fact, the number of standing waves tends to infinity as  $n_1 \rightarrow \infty$  [10]. For the nonlinear case, the term  $\gamma_1|u|^2$  effectively increases the dielectric constant of the cylinders. Therefore, it is possible to have an infinite sequence of nonlinear standing waves with increasing amplitudes.

For the results shown in Figs. 3 and 4, we use  $N = 13$  points to discretize each edge of the square  $\Omega$ ,  $4N = 52$  points to discretize the circle  $\partial D$  (i.e.  $r = a$ ), and  $M = 50$  points to discretize

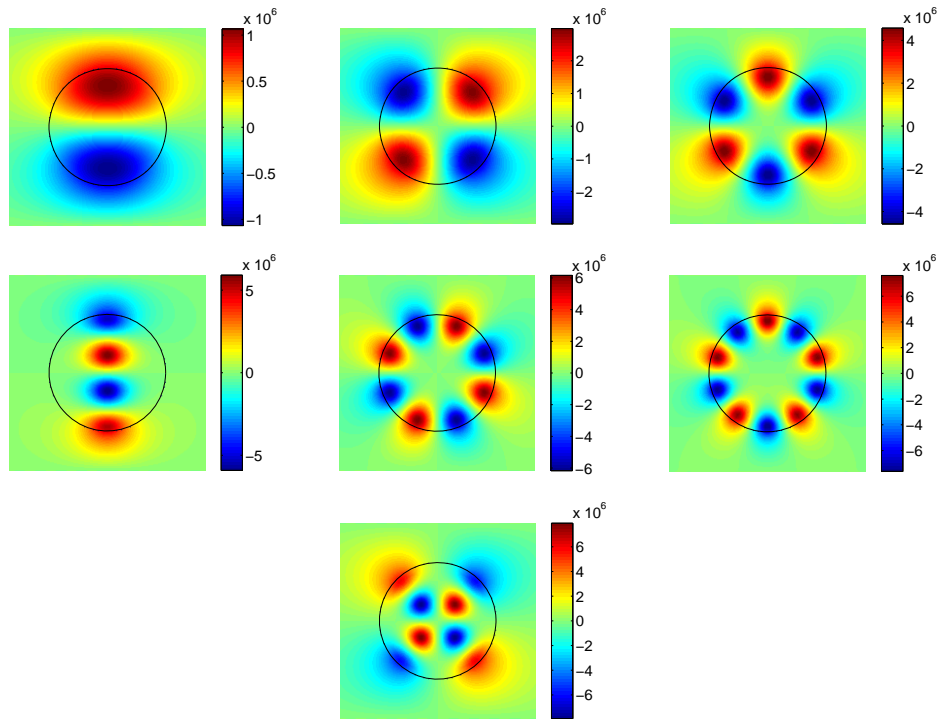


Fig. 4. Electric field patterns of the nonlinear standing wave fields corresponding to points A to G in Fig. 3.

the radial variable in the disk  $D$ . The symmetry properties with respect to  $x$  and  $y$  axes are also used to reduce the computation efforts.

### 5. Perturbation analysis

As we have seen in the previous section, for the array of cylinders being studied, two nonlinear standing waves are connected to the linear ones as the amplitude tends to zero. From Fig. 3, we observe that the relevant nonlinear standing wave only exists when  $\omega < \omega_*$ , where  $\omega_*$  is the angular frequency of a linear standing wave. Furthermore, it appears that the amplitude  $A$  is proportional to  $\sqrt{\omega_* - \omega}$ . In this section, we perform a perturbation analysis to confirm these observations and to provide a quantitative amplitude-frequency relation when the amplitude is small.

A linear standing wave is solution of the linear Helmholtz equation

$$\frac{\partial^2 \phi}{\partial x^2} + \frac{\partial^2 \phi}{\partial y^2} + k_0^2 n^2 \phi = 0, \quad (18)$$

subject to the periodic boundary condition in the  $y$  direction and the condition that  $\phi$  decays to zero as  $|x| \rightarrow \infty$ . This is an eigenvalue problem, where  $k_0$  (or  $k_0^2$ ) is the eigenvalue. Linear standing waves only exist at a discrete set of frequencies. Let  $\phi_0$  be a linear standing wave with the corresponding frequency  $\omega_*$  (free space wavenumber  $k_* = \omega_*/c$ ). The function  $\phi_0$  can be scaled by any constant. Without loss of generality, we assume  $\phi_0$  is real. To carry out a

perturbation analysis, we first write the nonlinear Helmholtz equation for a real  $u$  as

$$\frac{\partial^2 u}{\partial x^2} + \frac{\partial^2 u}{\partial y^2} + k_0^2 (n^2 + \gamma_1 F u^2) u = 0, \quad (19)$$

where  $F = F(x, y)$  is a function such that  $F = 1$  in the nonlinear cylinders and  $F = 0$  otherwise. This allows us to get rid of the small parameter  $\gamma_1$  by considering  $\sqrt{\gamma_1} u$  as the unknown function. We also need a small parameter proportional to  $(\omega_* - \omega)^{1/2}$ . For convenience, we use the small parameter  $\delta$  satisfying

$$\delta^2 = k_*^2 - k_0^2. \quad (20)$$

The nonlinear standing wave for a frequency slightly smaller than  $\omega_*$  can be expanded in an odd power series of  $\delta$  with the first term proportional to  $\phi_0$ . That is,

$$u = \frac{C\delta}{\sqrt{\gamma_1}} [\phi_0 + \delta^2 \phi_1 + O(\delta^4)], \quad (21)$$

where  $C$  is a constant to be determined.

Substituting expansion Eq. (21) into Eq. (19) and comparing the coefficients of  $\delta^3$  terms, we obtain the following equation for  $\phi_1$ :

$$\frac{\partial^2 \phi_1}{\partial x^2} + \frac{\partial^2 \phi_1}{\partial y^2} + k_*^2 n^2 \phi_1 = n^2 \phi_0 - C^2 k_*^2 F \phi_0^3. \quad (22)$$

Notice that  $\phi_1$  must satisfy the same periodic condition in  $y$  and must decay exponentially to zero as  $|x| \rightarrow \infty$ . To find the constant  $C$ , we multiply both sides of Eq. (22) by  $\phi_0$  and integrate on one period of the waveguide, i.e.,

$$S = \{(x, y) : -\infty < x < +\infty, |y| \leq L/2\}. \quad (23)$$

The left hand side gives a zero. Therefore,

$$C^2 = \frac{\int_S n^2 \phi_0^2 \, dx dy}{k_*^2 \int_D \phi_0^4 \, dx dy}. \quad (24)$$

In the above, we have used the property of  $F$  to reduce the integral in the denominator to an integral on disk  $D$ . The leading term of Eq. (21) gives

$$u \approx \frac{1}{\sqrt{\gamma_1}} \sqrt{1 - \left(\frac{\omega}{\omega_*}\right)^2} \left( \frac{\int_S n^2 \phi_0^2 \, dx dy}{\int_D \phi_0^4 \, dx dy} \right)^{1/2} \phi_0. \quad (25)$$

Notice that a scaling of  $\phi_0$  by any real number does not change the above result, and  $u$  is indeed proportional to  $\sqrt{\omega_* - \omega}$ , since

$$\sqrt{1 - \left(\frac{\omega}{\omega_*}\right)^2} \approx \sqrt{\omega_* - \omega} \sqrt{\frac{2}{\omega_*}}.$$

## 6. Conclusion

In this paper, nonlinear standing waves on a periodic array of circular cylinders with a Kerr nonlinearity are studied by a specially developed numerical method and a perturbation analysis. The standing waves are special nonlinear guided modes with a zero Bloch wavenumber and they exist above the lightline. While the linear standing waves only exist at a few distinct frequencies, the nonlinear standing waves exist for all frequencies in a given interval, and their amplitudes continuously depend on the frequency and blow up as the frequency approaches zero. It appears that for each frequency, there are infinite number of nonlinear standing waves. For a nonlinear standing wave connected to a linear one, a perturbation analysis provides an approximate amplitude-frequency relation when the amplitude is small.

Although we have only studied the  $E$  polarization for a special 2D structure with circular cylinders, we expect the conclusions are applicable to more general periodic waveguides, probably any 2D lossless periodic waveguide with a homogeneous surrounding medium and a reflection symmetry along the waveguide axis. Notice that the reflection symmetry guarantees the existence of linear standing waves [6, 10, 18]. The case of the  $H$  polarization is similar, because the only difference is a scaling of the boundary condition Eq. (12) by a constant.

To the best of our knowledge, it is the first time nonlinear standing waves are found on a periodic waveguide. Our study is based on the assumption that third (or higher) harmonic generation can be ignored. Similar to the studies on second harmonic generation [34, 35], the third harmonic may become important when some geometric conditions are satisfied. We believe it is worthwhile to further investigate the nonlinear solutions in a coupled system of equations for the fundamental frequency and third harmonic waves, to study the stability of these solutions and their nonlinear interactions with incident waves, and to explore their potential applications.

## Acknowledgments

This work was supported by the National Natural Science Foundation of China (11201508), the Scientific and Technological Research Program of Chongqing Municipal Education Commission (KJ130726), and the Research Grants Council of Hong Kong Special Administrative Region, China, under project CityU 11301914.